Science Advances
AAAS

advances.sciencemag.org/cgi/content/full/6/47/eabc9920/DC1

Supplementary Materials for

Dendritic and parallel processing of visual threats in the retina control defensive responses

T. Kim, N. Shen, J.-C. Hsiang, K.P. Johnson, D. Kerschensteiner*

*Corresponding author. Email: kerschensteinerd@wustl.edu

Published 18 November 2020, *Sci. Adv.* **6**, eabc9920 (2020)
DOI: 10.1126/sciadv.abc9920

The PDF file includes:

Other Supplementary Material for this manuscript includes the following:

(available at advances.sciencemag.org/cgi/content/full/6/47/eabc9920/DC1)

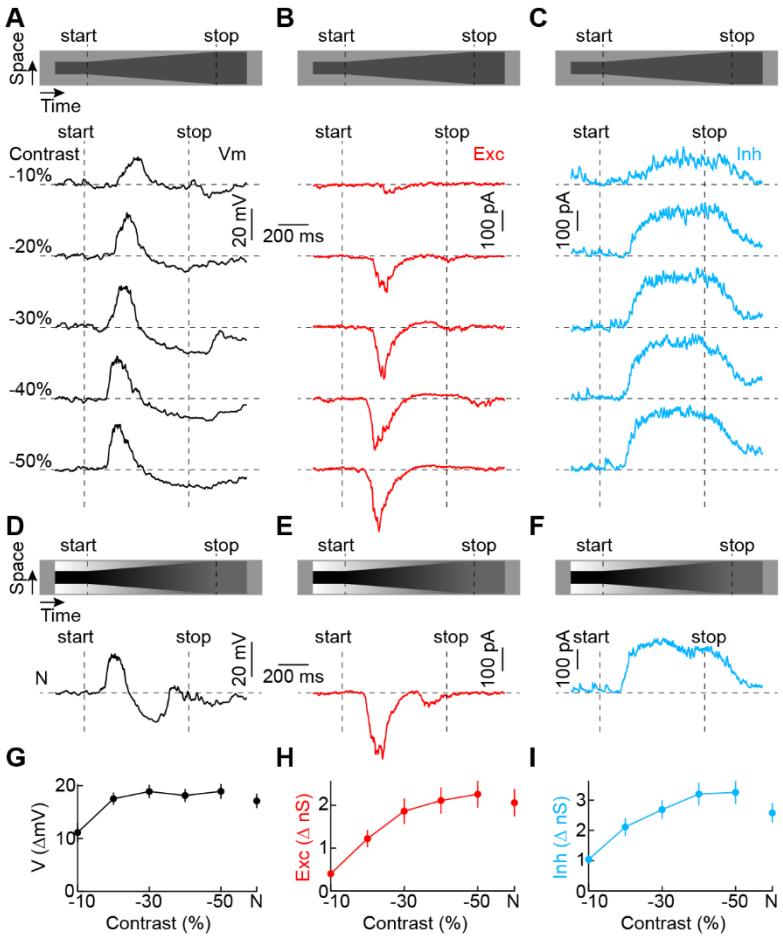

Figure S1. VG3 amacrine cell responses to looming of varying contrast and luminance-neutral approach motion. (**A** to **F**), Representative voltage (A and D), EPSC (B and E), and IPSC (C and F) traces recorded from VG3 amacrine cells during looming of increasing negative contrasts (A to C) or luminance-neutral approach motion (N, D to F). (**G** to **I**), Summary data for the voltage responses (G, n = 8 cells), and excitatory (H, n = 12 cells) and inhibitory (I, n = 12 cells) inputs elicited by looming of varying contrast and by luminance-neutral approach motion. For voltage responses, P = 0.0031 for the main effect of contrast by Friedman's test. Pairwise comparisons by Tukey-Kramer post-hoc analysis revealed significant differences only between -10% vs. -30% and vs. -50% contrast ($P < 0.02$). For excitation, $P = 2 \times 10^{-9}$ for the main effect of contrast. By Tukey-Kramer post-hoc analysis significant differences were observed for -10% vs. -30% to -50% and vs. N ($P < 0.02$), and -20% vs. -40%, vs. -50%, and vs. N ($P < 0.01$). For inhibition, $P = 2.6 \times 10^{-10}$ for the main effect of contrast. By Tukey-Kramer post-hoc analysis significant differences were observed for -10% vs. -30% to -50% and vs. N ($P < 0.02$), and -20% vs. -40% and vs. -50% ($P < 0.001$).

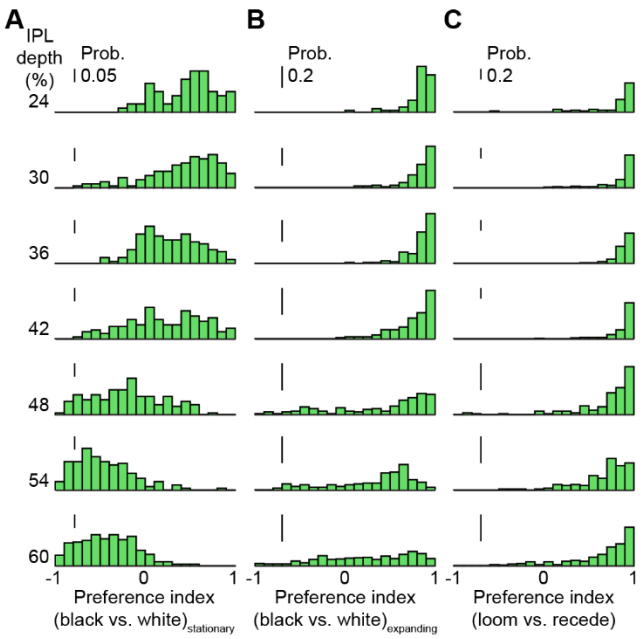

Figure S2. Distributions of stimulus preferences across VG3 dendrite arbors. (**A** to **C**), Distributions of stimulus preferences of VG3 dendrites (*VG3-Cre Ai148* mice) at different IPL depths for light decrements vs. increments in stationary disks (A, 100-μm diameter, 1.5 s ON, 1.5 s OFF), looming vs. white looming (B), and looming vs. receding (C). The numbers of ROIs at each depth were, 24%: n = 68, 30%: n = 138, 36%: n = 137, 42%: n = 153, 48%: n = 163, 54%: n = 162, 60%: n = 329).

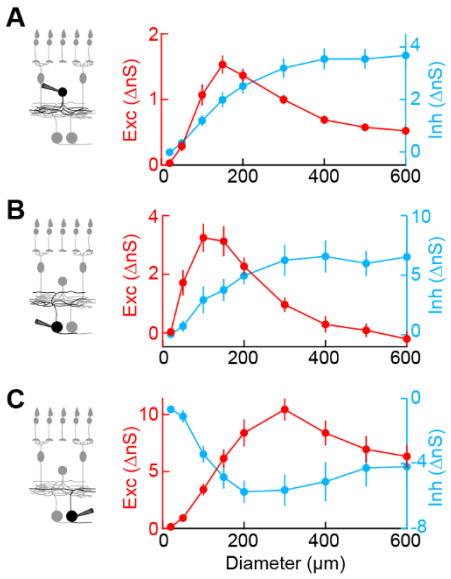

Figure S3. Excitatory and inhibitory receptive field architectures. (**A** to **C**), Summary data (mean ± SEM) of excitatory and inhibitory conductances activated by dark spots of varying diameter in VG3 amacrine cells (A, excitation: n = 26 cells, inhibition: n = 38 cells), W3 ganglion cells (B, excitation: n = 9 cells, inhibition: n = 8 cells), and OFFα ganglion cells (C, excitation: n = 8 cells, inhibition: n = 7 cells). We have previously published the VG3 amacrine cell data in this figure *(26)*.

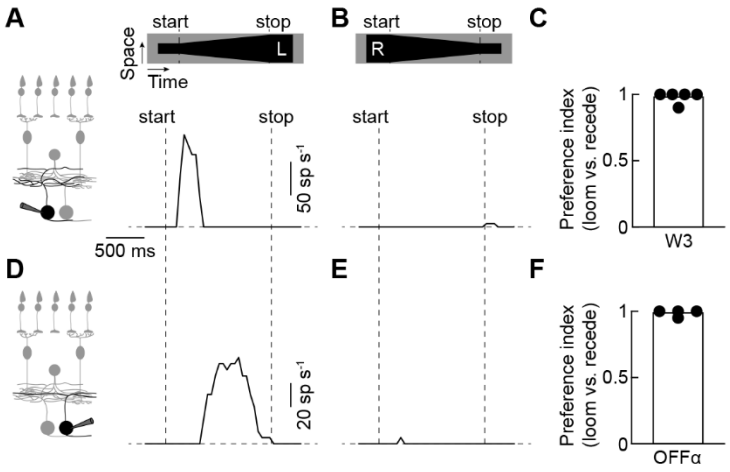

Figure S4. Looming preferences of W3 and OFFα ganglion cells. (**A** and **B**) Representative spike responses of a W3 ganglion cell to looming (A) and receding (B). (C) Summary data for the preference of W3 ganglion cells for looming vs. receding. (**D** to **F**) Analogous to (A to C) for OFFα ganglion cells.

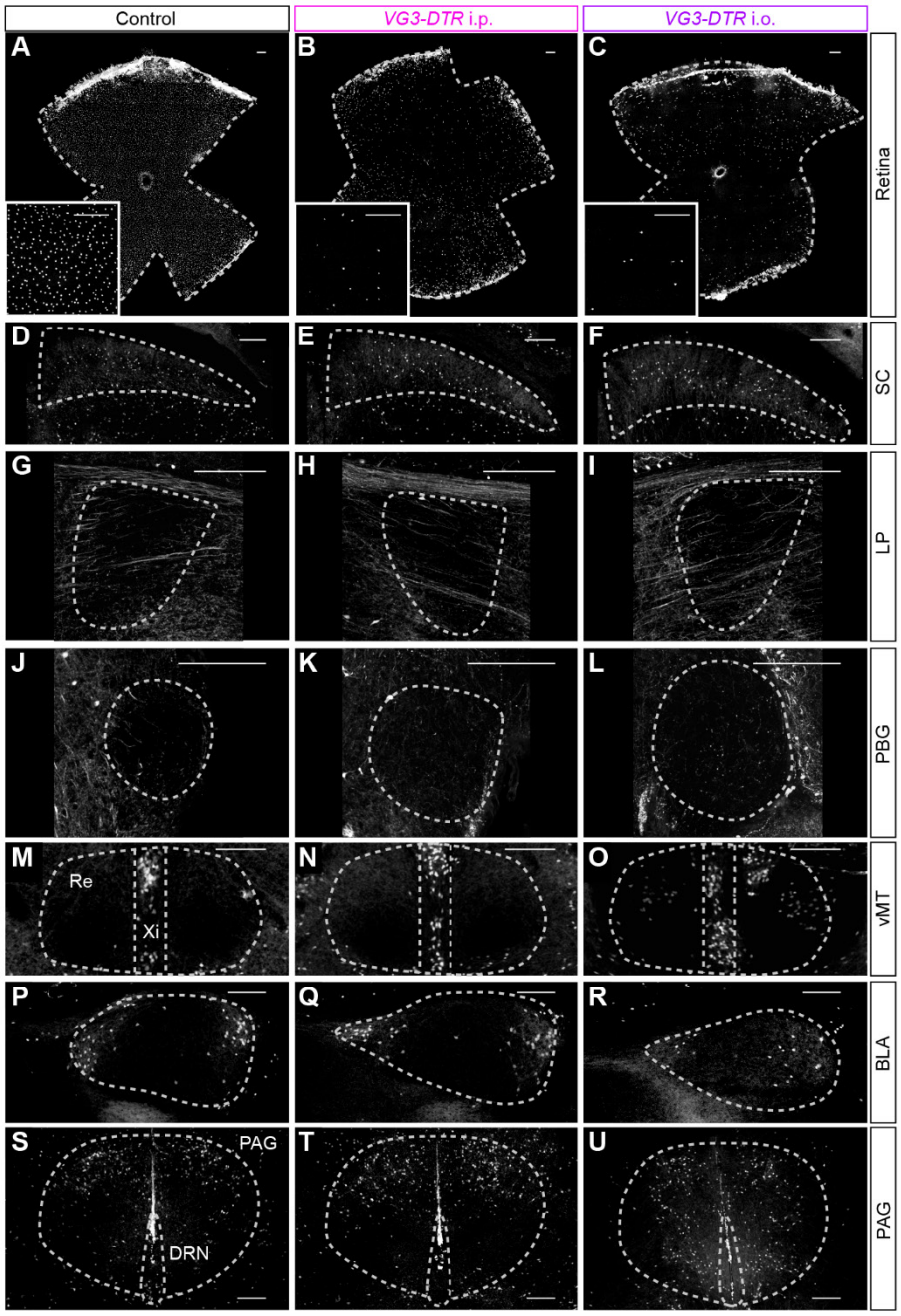

Figure S5. VG3 neurons in the brain are unaffected by DT injections in *VG3-DTR* mice. (**A** to **C**), Representative images of tdTomato-positive neurons in flat-mounted retinas of *VG3-Cre Ai9* (Ctrl), *VG3-DTR Ai9* mice two weeks after i.p. injection of DT (*VG3-DTR* i.p.), and *VG3-DTR* two weeks after i.o injection of DT (*VG3-DTR* i.o.). Insets show higher-magnification excerpts. (**D** to **F**), Analogous to (A to C) for VG3 neurons in the superior colliculus (SC). (**G** to **I**), Analogous to (A to C) for VG3 neurons in the lateral posterior nucleus of the thalamus (LP). (**J** to **L**), Analogous to (A to C) for VG3 neurons in the parabigeminal nucleus (PBG). (**M** to **O**), Analogous to (A to C) for VG3 neurons in the ventromedial thalamus (vMT) including nucleus reuniens (Re) and the xiphoid nucleus (Xi). (**P** to **R**), Analogous to (A to C) for VG3 neurons in the basolateral amygdala (BLA). (**S** to **U**), Analogous to (A to C) for VG3 neurons in the periaqueductal gray (PAG) and dorsal raphe nucleus (DRN).

Movie S1. Response of a wild-type mouse to looming. Representative response of a wild-type mouse to looming initiated when the mouse crosses the center of the arena.

Movie S2. Response of a wild-type mouse to receding. Representative response of a wild-type mouse to receding initiated when the mouse crosses the center of the arena.

Movie S3. Response of a wild-type mouse to white looming. Representative response of a wild-type mouse to white looming initiated when the mouse crosses the center of the arena.

Movie S4. Response of a control mouse injected with DT i.p. to looming. Representative response of a control (i.e., *VG3-Cre*) mouse injected with DT i.p. to looming initiated when the mouse crosses the center of the arena.

Movie S5. Response of a control mouse injected with DT i.o. to looming. Representative response of a control (i.e., *VG3-Cre*) mouse injected with DT i.o. to looming initiated when the mouse crosses the center of the arena.

Movie S6. Response of a *VG3-DTR* mouse injected with DT i.p. to looming. Representative response of a *VG3-DTR* mouse injected with DT i.p. to looming initiated when the mouse crosses the center of the arena.

Movie S7. Response of a *VG3-DTR* mouse injected with DT i.o. to looming. Representative response of a *VG3-DTR* mouse injected with DT i.o. to looming initiated when the mouse crosses the center of the arena.